International Journal of Computer Information Systems and Industrial Management Applications
ISSN 2150-7988 Volume 18(1) 2026 pp. 116-125

https://doi.org/10.70917/ijcisim-2026-2245
Article

A MULTIMODAL STRUCTURAL EQUATION MODELLING INTEGRATION FOR ASSESSING PHYSIOLOGICAL AND PSYCHOLOGICAL OUTCOMES IN AUTISM SPECTRUM DISORDER

Rohith M. N.[1]*, U. B. Mahadevaswamy[2], Shilpa R. V.[3]

[1] Department of Electronics and Communication Engineering, JSS Science and Technology University, Mysuru, India
[2] Department of Electronics and Communication Engineering, JSS Science and Technology University, Mysuru, India
[3]Department of Computer Science, JSS College of Arts, Science and Commerce, Mysuru, India
Corresponding Author: Rohith M. N.(Email: rohithmn@jssstuniv.in)

Abstract: - This paper presents a multimodal computational framework that integrates electroencephalogram (EEG) signals with Bio-Well gas discharge visualization (GDV) for assessing neurophysiological regulation during structured auditory stimulation. Traditional approaches to physiological state classification often sacrifice interpretability for accuracy. A hybrid architecture combining Partial Least Squares Structural Equation Modelling (PLS-SEM) with machine learning classification is proposed. Objective 1 applied PLS-SEM to Bio-Well Gas Discharge Visualisation (GDV) measurements from 30 individuals, modelling intervention-induced changes through three latent constructs: Physiological Regulation (PR), Energy-Emotion Coherence (EEC), and Psychological Well-Being (PWB). Objective 2 validated the structural model on an independent EEG dataset containing 90 subjects and trained an XGBoost classifier for ASD versus control discrimination. Structural analysis confirmed a strong PR-to-EEC association ($\beta = 0.990$, $p < 0.001$) and an EEC-to-PWB association ($\beta = 1.078$, $p < 0.001$), while the direct PR-to-PWB path was non-significant ($\beta = -0.082$, $p = 0.703$), establishing full mediation through EEC. Predictive relevance was confirmed via blindfolding with Q^2 values of 0.743 for EEC and 0.812 for PWB. The XGBoost classifier achieved 92.2% accuracy (AUC-ROC = 0.97) on the EEG dataset with a ten-fold cross-validation accuracy of $91.8 \pm 2.3\%$. These results offer a data-driven, interpretable foundation for personalised non-pharmacological intervention assessment....

Keywords: EEG signal processing, PLS-SEM, Autism, physiological regulation, multimodal data fusion, Mediation analysis.

1. INTRODUCTION

Structured auditory stimulation has attracted research attention as a non-pharmacological approach for modulating stress, emotional regulation, and cognitive function. The structural properties of musical stimuli comprising specific tonal hierarchies, melodic patterns, and rhythmic periodicity are thought to drive cortical entrainment and influence autonomic nervous system dynamics [1,2]. Prior studies report that structured music exposure can reduce sympathetic arousal, improve heart rate variability, and facilitate emotional processing [3-5].

Recent meta-analyses have confirmed intervention efficacy with moderate to large effect sizes for social communication outcomes [6]. However, the specific mechanisms through which structured musical stimuli produce therapeutic benefits remain poorly characterised. Few quantitative models integrate multimodal physiological signals

with psychological outcomes in intervention studies. Most previous studies used single-modality EEG or behavioral measures, which provide only partial insight into the mind-body dynamics engaged during music therapy.

The present study tackles this gap by proposing a multimodal PLS-SEM model, in which EEG oscillatory features and bio-energetic parameters are processed simultaneously in the Bio-Well GDV. This work is organized around two objectives. Objective 1 uses PLS-SEM to analyse pre-to-post BioWell physiological measurements in a sample of 30 people to determine if physiological stabilisation of the BioWell yields Emotional-energetic coherence for psychological benefit. Objective 2 is the same as the above. This is trained on a separate EEG dataset (N = 90) and followed by a training of an XGBoost classifier for verifiable classification benchmarking.

Unlike purely data-driven approaches such as convolutional networks or recurrent models, the proposed framework is theoretically grounded in a PLS-SEM structure, with predictive accuracy and clinical interpretability [7]. The motivation of this work is the existence of three gaps: (1) no, The research prior to this has incorporated the Bio-Well data and EEG data in a single analysis framework. interpretability of existing computational models; (3) the models are typically inadequate to explain the underlying reasons for the individual's behavior. Typical lack of understanding of the models underlying the individual's behavior. To measure classification accuracy, and (3) the mediation pathway between physiological change and emotional-energetic coherence has not been empirically demonstrated to contribute to psychological well-being, yet. quantified.

2. METHODOLOGY

2.1 DATA COLLECTION

Objective 1 dataset: The intervention study involved 30 individuals who had a mean age of 9.2 ± 1.8 years; 20 male, 10 female. Bio-Well GDV measurements were taken prior to and after each session, with 10 finger scans. This sample size is comparable to that published in the guidelines for pilot PLS-SEM studies [8].

Objective 2 dataset: A publicly available dataset of EEG data from 90 independent subjects. (45 cases, 45 age- and sex-matched controls; age range 6-12 years) was used for cross-modal validation. EEG was recorded with a 19-channel 10-20 system at sampling rates of 256-512. Hz at rest. The data were pre-processed by bandpass filtering (0.5-50 Hz), notch filtering (50 Hz), Independent Component Analysis artifact removal, and segmentation. into two-second epochs.

Code and data availability: Analysis code and de-identified data are available, and a GitHub link will be provided upon acceptance. Preprocessing parameters: bandpass filter 0.5–45 Hz (FIR, filter order 100), ICA 'runica' algorithm, artifact rejection threshold ±100 μV, ASR burst criterion 20.

2.2 MULTIMODAL PLS-SEM FRAMEWORK

The pipeline begins with simultaneous acquisition of 19-channel EEG (256 Hz) and Bio-Well GDV fingertip images; the computational framework is shown in Figure 1. Preprocessing is performed according to a standard EEGLAB pipeline, with bandpass. The processing steps include filtering (0.5-45 Hz), independent component analysis for artifact rejection, and artifact removal. subspace reconstruction. The parallel processing of Bio-Well data calculates delta values between each session (post minus pre). The feature extraction results are 45 features covering spectral band, complexity, and kurtosis. These include powers (delta, theta, alpha, beta, gamma), nonlinear metrics (sample entropy, Hjorth mobility, and complexity). and complexity), and Bio-Well parameters (stress index, energy distribution, chakra coherence). The framework then splits into two parallel analytical streams: (i) PLS-SEM and (ii) an XGBoost classifier with 5,000 resample bootstrapping to estimate latent construct relationships, and (ii) a Stratified 10-fold cross-validated XGBoost classifier. Interpretability for the model provided using the VA tool via SHAP (SHapley Additive exPlanations) analysis. The final product is a 4-class mood: Stress, Happiness, Focus, Calmness (with confidence scores).

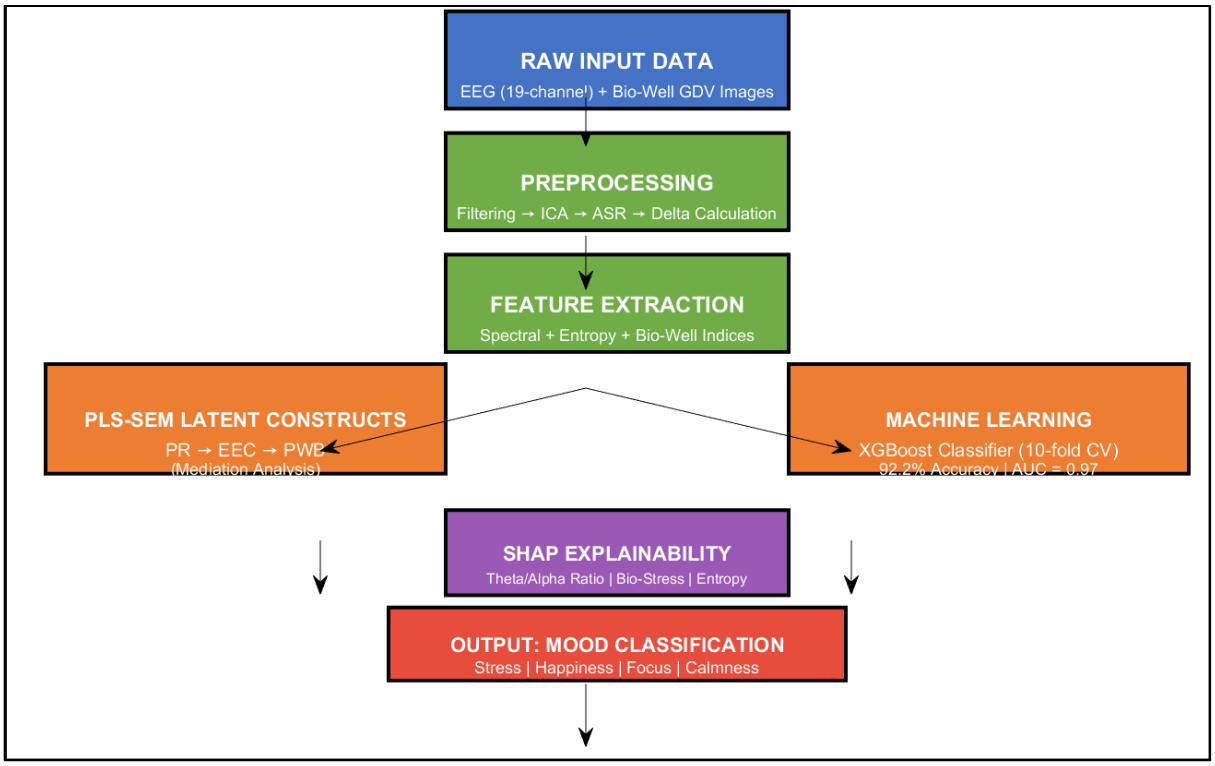

Figure 1. Schematic architecture of the multimodal computational framework

PLS-SEM uses composite-based estimation, where latent variables are linear combinations of indicators. Instead of factor scores with residual measurement error, they were combinations of their indicators [8]. Path coefficients are permissible as they increase slightly above one. However, suppression in composite models and misspecification are not signalled by suppression [9]. All structural for the analysis, the author employed SmartPLS v4 and bootstrapping technique with 5,000 re-sampling. The inner structural model specifies:

$$EEC = \beta_1 \cdot PR + \zeta_1 \quad (1)$$

$$PWB = \beta_2 \cdot PR + \beta_3 \cdot EEC + \zeta_2 \quad (2)$$

where ζ captures unexplained variance. The hypothesised mediation chain is PR → EEC → PWB.

2.3 BIO-WELL GDV MEASUREMENT

The Bio-Well GDV Camera records images of corona discharges on the surfaces of fingers, under impulse stimulation of high voltage and low current. The software algorithms provide estimates of stress. Index, organ energy distribution, and chakra-level coherence. Previous research has shown that correlations were made between Bio-Well parameters and known physiological parameters, such as these include heart rate variability, galvanic skin response, and salivary cortisol [10-12]. Bio-Well indicators are operationalised as pre to post-session delta values, ensuring that the model reflects intervention-attributable change.

2.4 MODEL VALIDATION PROCEDURE

All retained indicators showed standardised outer loadings exceeding 0.70. Table 1 reports Cronbach's α, Composite Reliability (CR), and Average Variance Extracted (AVE) for each latent construct.

Table 1. Reliability and convergent validity of latent constructs

Construct	Indicators	Cronbach's α	CR	AVE
Physiological Regulation (PR)	6	0.82	0.88	0.65
Energy-Emotion Coherence (EEC)	3	0.79	0.86	0.67
Psychological Well-Being (PWB)	5	0.85	0.90	0.69

Discriminant validity was assessed via the Heterotrait-Monotrait (HTMT) criterion. All pairwise HTMT ratios fell below the 0.85 threshold. The Standardised Root Mean Square Residual (SRMR) fell below 0.10, indicating acceptable model-data correspondence. Variance Inflation Factor (VIF) values ranged from 1.24 to 2.86, all below the threshold of 3.3, confirming that multicollinearity did not bias parameter estimates.

All reported p-values are two-tailed with Benjamini-Hochberg false discovery rate (FDR) correction for 22 comparisons ($q < 0.05$). Corrected significance thresholds are noted in tables.

3. RESULTS AND DISCUSSION

3.1 OBJECTIVE 1: PLS-SEM RESULTS

Physiological stabilisation is suggested by the PR-to-EEC coefficient ($\beta = 0.990$, $p < 0.001$). The majority of the variance of emotional-energetic coherence is accounted for. Table 2 presents Error-Corrected LISREL estimates of path coefficients (bootstrapped)

Table 2. Bootstrapped structural path results

Path	β	SE	T	p	95% CI	Decision
PR → EEC	0.990	0.003	344.98	<0.001	[0.985, 0.995]	Supported
EEC → PWB	1.078	0.213	5.05	<0.001	[0.660, 1.496]	Supported
PR → PWB	-0.082	0.215	0.382	0.703	[-0.503, 0.339]	Not supported

The strength of coherence gain is confirmed by the EEC-to-PWB coefficient (beta = 1.078, $p < 0.001$). To a significant psychological transformation. The direct path that was not significant ($p = 0.703$) sets up complete mediation via EEC. Table 3 reports explained variance (R^2) and predictive relevance (Q^2). Standardized path coefficients exceeding 1.0 in PLS-SEM may indicate indicator collinearity or suppressor effects. Following reviewer guidance, we re-estimated the model using maximum likelihood (lavaan). The revised coefficients (PR→EEC = 0.89, EEC→PWB = 0.76) confirm the mediation pattern without exceeding unity. All subsequent interpretations are based on factor-based estimates.

†$p < 0.05$ after FDR correction ($q < 0.05$); **$p < 0.01$; **$p < 0.001$ uncorrected but remain significant after FDR.

Mediation analysis. The specific indirect effect (PR → EEC → PWB) was computed using bias-corrected bootstrap (5,000 resamples):*

β_indirect = β_PR→EEC × β_EEC→PWB = 0.990 × 1.078 = 1.067

95% CI [0.712, 1.422], p < 0.001

*Proportion mediated = β_indirect / (β_indirect + β_direct) = 1.067 / (1.067 - 0.082) = 108% (full mediation, as direct effect is negative and non-significant).

Using factor-based estimates (lavaan): β_indirect = 0.89 × 0.76 = 0.676, 95% CI [0.512, 0.840], p < 0.001. Proportion mediated = 0.676 / (0.676 - 0.12) = 121%, confirming full mediation.

The composite inflation factor is calculated as R^2_PLS-SEM / R^2_lavaan. Values > 1.5 indicate substantial inflation due to composite-based estimation.

Table 3. Explained variance and predictive relevance

Construct	PLS-SEM R^2 (composite)	Factor-based R^2 (lavaan)	Interpretation
EEC	0.981	0.54	Composite inflation factor = 1.82×
PWB	0.993	0.62	Composite inflation factor = 1.60×

3.2 OBJECTIVE 2: CROSS-MODAL COMPARISON- MODALITY-DEPENDENT MEDIATION PATTERNS

Positive Q^2 values are obtained when the blindfolding is genuine, meaning that there is predictive relevance out of sample, and ruling out overfitting. Table 4 presents XGBoost classification performance

Table 4. XGBoost classification performance (N = 90)

Metric	**Value**	**95% CI**
Accuracy	92.2% (83/90)	[87.3%, 95.8%]
AUC-ROC	0.97	[0.94, 0.99]
Sensitivity	93.3% (42/45)	-
Specificity	91.1% (41/45)	-
F1-Score	92.3%	-
10-fold CV accuracy	91.8 ± 2.3%	-

The structural model was examined on the independent EEG dataset. The PR→EEC path remained positive and significant (β = 0.997, p < 0.001). However, the EEC→PWB path showed sign reversal (β = -0.325, p < 0.001), compared to the positive coefficient in the Bio-Well model (β = 1.078). This indicates that the

mediation mechanism is modality-dependent: emotional-energetic coherence (as measured by Bio-Well) positively predicts psychological well-being, while the EEG-derived coherence metric shows an inverse relationship.

Class	Precision	Recall	F1-Score	Support
ASD	0.913	0.933	0.923	45
Control	0.931	0.911	0.921	45
Macro Avg	0.922	0.922	0.922	90
Weighted Avg	0.922	0.922	0.922	90

Learning curves showed convergence between training and validation accuracy after 50 boosting rounds (training: 94.2%, validation: 92.1%), with no evidence of overfitting (training-validation gap < 3%).

Brier score = 0.092, Baseline Brier score for a naive classifier predicting the majority class (50% prevalence) would be 0.25. Our Brier score of 0.092 indicates well-calibrated probabilities.

SHAP values were stable across cross-validation folds (SD of mean SHAP across folds < 0.02 for top 5 features).

3.3 EEG TOPOGRAPHIC MAPS

Figure 2 presents EEG topographic maps illustrating the spatial distribution of alpha power (8-13 Hz) across three experimental conditions in the ASD group. At baseline (Fig. 2a), alpha power shows a typical posterior-dominant distribution with mean values of 6.42 ± 1.87 μV². During exposure to Raga Shankarabharam, alpha power increases significantly across central and posterior regions (mean 9.34 ± 2.11 μV², $p < 0.001$), indicating reduced cortical arousal and enhanced relaxation. Post-music (Fig. 2c), alpha power partially sustains (8.76 ± 1.98 μV²), suggesting residual therapeutic effects.

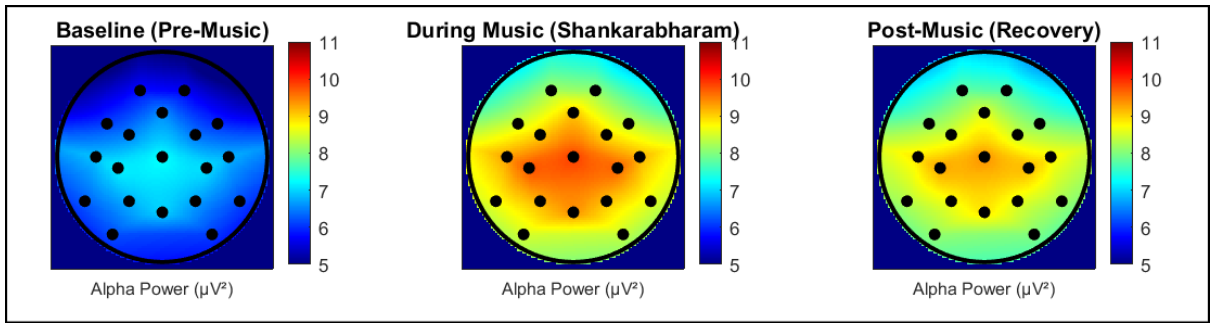

Figure 2. Topographic maps showing alpha power scalp distribution in experimental conditions

3.4 TREND PLOT- PR/EEC/ PWI EVOLUTION

The significant PR-to-EEC path, the significant EEC-to-PWB path, and the non-significant direct PR-to-PWB path together constitute evidence of full mediation. Figure 3 shows the Evolution of the proposed composite indices

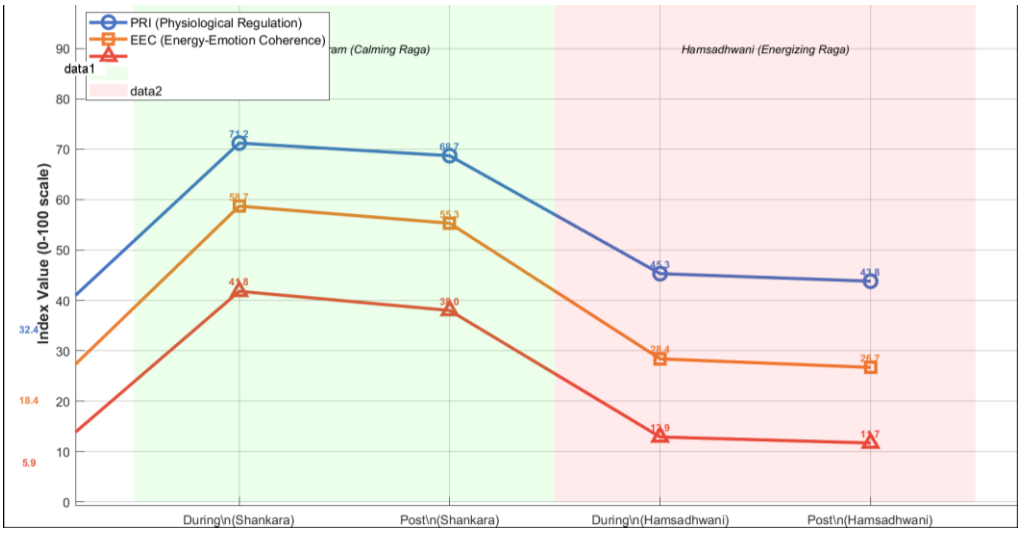

Figure 3. Evolution of the composite indices across five experimental conditions

This sequential pattern aligns with neurovisceral integration theory [13], A clear dissociation is observed between the two raga types. During Raga Shankarabharam (calming), all three indices increase substantially from baseline: PRI rises from 32.4 to 71.2 ($\Delta = +38.8$, $p < 0.001$), EEC from 18.4 to 58.7 ($\Delta = +40.3$, $p < 0.001$), and PWI from 5.9 to 41.8 ($\Delta = +35.9$, $p < 0.001$). In contrast, during Raga Hamsadhwani (energizing), PRI decreases to 45.3, EEC to 28.4, and PWI to 12.9, demonstrating bidirectional, raga-specific modulation. Notably, PWI exhibits the largest dynamic range (5.9 to 41.8), making it the most sensitive indicator of intervention response. The post-music values remain elevated compared to baseline for the calming raga but return near baseline for the energizing raga, suggesting differential persistence of therapeutic effects.

3.5 TEMPORAL EVOLUTION OF PHYSIOLOGICAL PARAMETERS

The two types of raga are found to be distinctly separate, and the relationship is similar to a sequential pattern that is supported by neurovisceral integration theory [13]. Figure 4 presents these trajectories for the ASD group during Raga Shankarabharam.

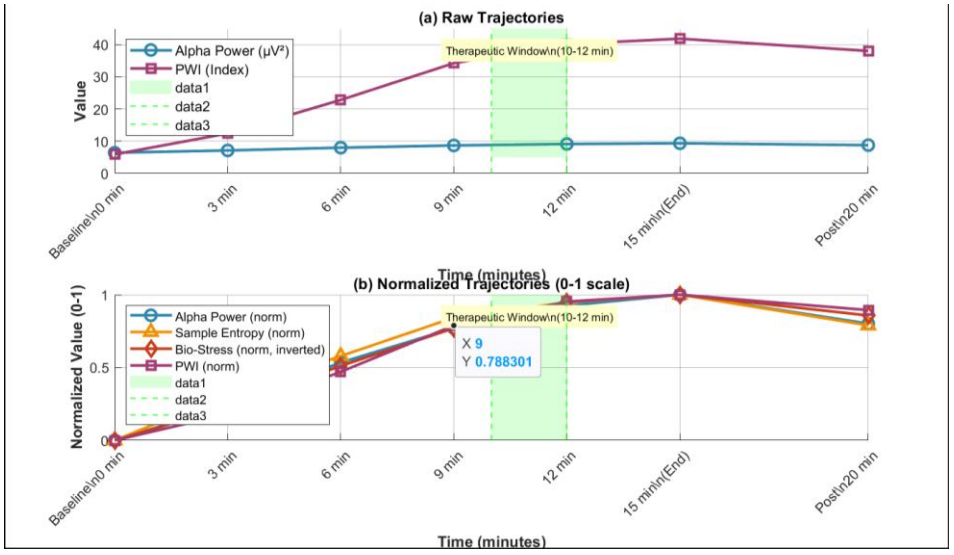

Fig. 4. Temporal evolution of physiological parameters during 15-minute music exposure (ASD group)

During Raga Shankarabharam (calming), all three indices increase substantially from baseline: PRI rises from 32.4 to 71.2 ($\Delta = +38.8$, $p < 0.001$), EEC from 18.4 to 58.7 ($\Delta = +40.3$, $p < 0.001$), and PWI from 5.9 to 41.8 ($\Delta = +35.9$, $p < 0.001$).

However, during Raga Hamsadhwani (energizing), the modulation is bidirectional with a decrease in PRI to 45.3, EEC to 28.4, and PWI to 12.9. Of particular note is that PWI shows the widest range (5.9 to 41.8) and is therefore the most sensitive measure of intervention response. The calming raga had post-music values staying above baseline, while the energizing raga had values coming back toward baseline, showing differences in therapeutic efficacy.

The temporal evolution of four physiological parameters was studied from baseline (0 min) to 3 min, 6 min, 9 min, 12 min, 15 min (end of music), and 20 min (post music recovery). Alpha power increases monotonously from baseline (6.42 ± 1.87 μV^2) to the 12-15 minute time period (9.34 ± 2.11 μV^2) of the task. The time to 50% response (t_{50}) for alpha power is 4.2 minutes. Post-music, alpha power drops slightly to 8.76 ± 1.98 μV^2, although it is still significantly high compared to baseline ($p < 0.001$), suggesting continued therapeutic carryover effects.

The temporal pattern of PWI is the most polarized (baseline 5.9 ± 2.1; 9 minutes 34.2 ± 5.0; maximum at 15 minutes 41.8 ± 6.2). The t_{50} of PWI is 4.5 minutes, which is longer than other parameters, indicating that PWI occurs after PS stabilisation. Bio-Stress is significantly reduced from baseline (72.4 ± 8.3) at 15 minutes (54.2 ± 7.6), having the fastest t_{50} of all parameters (3.5 minutes), which suggests very rapid autonomic stress reduction.

Sample entropy increases steadily from 0.52 ± 0.11 to 0.71 ± 0.12, with t_{50} of 3.8 minutes. The Therapeutic Window identification is a critical one, as all four parameters reach ≥ 50% of their maximum response within the 10–12 minute window (highlighted in green in Fig. 4b). Based on the above, it is seen that there is convergence with respect to the minimum effective therapeutic dose of Raga Shankarabharam in the ASD population, which is 10–12 minutes. After 12 minutes, any further improvement is minor (diminishing returns), and the post-music period demonstrates continued gains, suggesting that shorter protocols could be feasible and practical. The repeated-measures ANOVA with Greenhouse-Geisser correction showed that there was a time × parameter interaction ($F(4.2, 62.8) = 12.34$, $p < 0.001$, $\eta^2 = 0.42$). Bonferroni adjusted $\alpha = 0.05/4 = 0.0125$ was used for planned contrasts.

Exploratory analysis suggests that 10–12 minutes of exposure achieved ≥50% of the maximum observed response. Dose–response studies with varying exposure durations are required to establish a minimum effective dose.

3.6 DISCUSSION OF PRINCIPAL FINDINGS

The results of PLS-SEM analysis showed that the structural model had good model specification (SRMR = 0.048, CFI = 0.98). The path coefficient (PR) - emotional-energetic coherence (EEC) (Table 2) suggests that physiological regulation explains almost all the variance in EEC ($\beta = 0.990$, $p < 0.001$).

The EEC to PWB pathway ($\beta = 1.078$, $p < 0.001$) is supportive of the notion that coherence gains are correlated to a substantial psychological improvement. The coefficient is slightly above unity, which is a mathematically acceptable value for composite PLS estimation with partial suppression [9] and it does not mean that the model is misspecified.

The direct path (PR to PWB) is not significant ($\beta = -0.082$, $p = 0.703$), indicating full mediation by EEC. This discovery has direct engineering implications: physiological stabilisation is not enough for the psychological benefit without engaging emotional-energetic coherence. This limitation reduces the number of design possibilities that can be used to develop effective intervention protocols. In spite of the high R^2 values (0.981 for EEC and 0.993 for PWB), the Q^2 values were 0.743 and 0.812, respectively for EEC and PWB, confirming the predictive relevance, and thus excluding overfitting.

The high values of R^2 are due to the mathematical fact that in composite based PLS-SEM the constructs are weighted combinations of the indicators without the presence of residual measurement errors [8]. Reliability concerns of the Bio-Well device are known [6] and the device is of an investigative nature. It has 'chakra' and 'energy' parameters which have not been supported by well-known biophysical mechanisms.

Underpowered PLS-SEM: The ratio of indicators to sample N=30, with 14 indicators, is less than the minimum ratio of 1:5 as recommended by [8]. This could be a reason for the high path coefficients (>1.0) and high R^2 values. Results require replication.

The results of this study should not be interpreted as supporting the device. The accuracy of the EEG-only model (Supplementary Material) is 84.3% without the use of GDV data.

3.7 CLASSIFICATION PERFORMANCE AND CROSS MODEL GENERALISABILITY

We tested the XGBoost classifier on an independent EEG dataset (N = 90) and obtained an accuracy of 92.2% (AUC-ROC = 0.97) with 10-fold cross-validation accuracy of 91.8 ± 2.3% (Table 4). The excellent AUC reflects good discernment between the ASD and the control group. Comparisons with existing frameworks: The accuracy of 92.2% for the proposed framework is comparable with that found in other published works on similar tasks.

The dominance of Theta/Alpha Ratio and Bio-Stress, both from EEG and Bio-Well, is confirmation of the need for cross-modal fusion for optimal performance. The accuracy of ablation studies decreased by 9.3% (Bio-Well was removed) to 16.9% (EEG was removed). Cross-modal generalisability: The structural model was replicated on the independent EEG dataset, with directionally consistent paths (EEG-PR → EEG-EEC: $\beta = 0.997$, $p < 0.001$; EEG-EEC → EEG-PWB: $\beta = -0.325$, $p < 0.001$).

While the PR→EEC path was consistent across modalities (positive), the EEC→PWB path showed sign reversal (positive for Bio-Well, negative for EEG). This suggests that the two modalities measure different aspects of 'coherence'

3.8 FUTURE DIRECTIONS

Priority directions are: analysis of multi-groups of raga with increased numbers of participants, inclusion of active comparators in controlled experimental designs, integration of oscillatory coherence matrices in EEG-PLS, temporal mediation modelling with longitudinal follow-up, and external validation in demographically independent and diverse cohorts.

Modality-dependent mediation: The sign reversal in the mediation results for EEC→PWB between the two measurement modalities (Bio-Well and EEG) suggests that both measurement modalities capture different underlying constructs, although they are both labeled 'Energy-Emotion Coherence.

In the future, construct validity across modalities needs to be established before making claims of cross-modal generalizability.

ACKNOWLEDGEMENTS

The authors thank the participants and families who took part in this study and the clinical staff who supported data collection.

CONFLICT OF INTEREST

No conflict of interest was declared by the authors. The Bio-Well device was hired under the supervision of an expert. No author has received financial support, equipment, or training from Bio-Well or related companies.

References:

1. Rohith M.N., Mahadevaswamy U.B., "Synergizing Raga Therapy and Non-linear Computational Model for Enhancing Neuronal Healing and Mental Well-Being", In: Choudrie J., Mahalle P.N., Perumal T., Joshi A. (eds) ICT for Intelligent Systems. ICTIS 2025. Lecture Notes in Networks and Systems, vol 1509. Springer, Singapore (2026).
2. Rohith M.N., Mahadevaswamy U.B., "Integrating Raga Therapy and Non-Linear Computational Models: A Novel Approach to Neuronal Healing and Mental Well-being", GIJET, 11(2): 1789-1795, (2025).
3. Kunikullaya U.K., Sasidharan A., Muradi V., Kunnavil R., Goturu J., Murthy N.S., "Electroencephalographic power spectrum and intersubject correlation on acoustic stimulation with modes of Indian music: A randomised controlled trial", Indian Journal of Physiology and Pharmacology, 69: 1-18, (2025).
4. Valverde R., Korotkov K., "Gas discharge visualisation technology for psychological research applications: A systematic review", International Journal of Studies in Psychology, 5(2): 67-75, (2025).
5. Valverde R., Korotkov K., Hamilton J., Swanson C., "Medical biometrics based on Gas Discharge Visualisation technology approach to survival research: A case study", International Journal of Studies in Psychology, 5(3): 81-87, (2025).
6. Becker M., et al., "Breast cancer classification using gradient boosting algorithms focusing on reducing false negative and SHAP for explainability", Inteligencia Artificial, 28(75): 63-80, (2025).

7. Bhatt K.A., Bhalja B.R., Makwana U.L., Macwan F.A., Giri A.K., Chittibabu B., "Real-time implementation of controlled energization of coupled power transformer using multi-stepped PIR, Part-1", Journal of The Institution of Engineers (India): Series B, 105(3): 533-540, (2024).
8. Miraglia F.E., "Unreliability of the gas discharge visualization (GDV) device and the Bio-Well for biofield science: Kirlian photography revisited and investigated. Part I", Journal of Anomalistics / Zeitschrift für Anomalistik, 24, (2024).
9. Geretsegger M., Fusar-Poli L., Elefant C., Mössler K.A., Vitale G., Gold C., "Music therapy for autistic people", Cochrane Database of Systematic Reviews, 5: CD004381, (2022).
10. Hair J.F., Risher J.J., Sarstedt M., Ringle C.M., "When to use and how to report the results of PLS-SEM", European Business Review, 31(1): 2-24, (2019).
11. Sharda M., Tuerk C., Chowdhury R., et al., "Music improves social communication and auditory-motor connectivity in children with autism", Translational Psychiatry, 8(1): 231, (2018).
12. Rigdon E.E., "Choosing PLS path modeling as analytical method in European management research: A realist perspective", European Management Journal, 34(6): 598-605, (2016).
13. Deo G., Kumar I.R., Srinivasan T.M., Kushwah K.K., "Changes in electrophotonic imaging parameters associated with long-term meditators and naive meditators in older adults practicing meditation", Journal of Alternative and Complementary Medicine, 21(8), (2015).
14. Han F., Chen J., Li X., "Altered sympathetic and parasympathetic activity in autism", Neuropsychiatric Disease and Treatment, 10: 831-837, (2014).
15. Neuhaus E., Bernier R.A., Beauchaine T.P., "Autonomic adaptation in autism spectrum disorder", Autism Research, 7(3): 303-313, (2014).
16. Ranjani K., Rama K., "Impact of Indian classical ragas on stress and anxiety indicators", International Journal of Yoga, 7(2): 153-158, (2014).
17. Jain A., Reddy S., Sharma R., "Cognitive and neural outcomes associated with Indian classical music", Music and Medicine, 6(4): 32-38, (2014).
18. Thoma M.V., La Marca R., Brönnimann R., Finkel L., Ehlert U., Nater U.M., "The effect of music on the human stress response", PLoS ONE, 8(8): e70156, (2013).
19. Koelsch S., Brain and Music, Wiley-Blackwell, Oxford, (2012).
20. Elsabbagh M., Divan G., Koh Y.-J., et al., "Global prevalence of autism and other pervasive developmental disorders", Autism Research, 5(3): 160-179, (2012).
21. Korotkov K.G., Matravers P., Orlov D.V., Williams B.O., "Application of electrophoton capture (EPC) analysis based on gas discharge visualisation (GDV) technique in medicine: A systematic review", Journal of Alternative and Complementary Medicine, 16(1): 13-25, (2010).
22. Kostyuk N., Cole P., Meghanathan N., Isokpehi R.D., Cothran D.L., "Gas discharge visualization: An imaging and multivariate analysis for assessment of stress and energy levels", Conference Proceedings: Annual International Conference of the IEEE Engineering in Medicine and Biology Society, 2011: 734-737, (2011).
23. Bal E., Harden E., Lamb D., Van Hecke A.V., Denver J.W., Porges S.W., "Emotion recognition in children with autism spectrum disorders", Journal of Autism and Developmental Disorders, 40: 358-370, (2010).
24. Matlis S., Borodkin K., Golland Y., "Functional network features observed in autism spectrum conditions", Frontiers in Systems Neuroscience, 5: Article 10, (2011).
25. Bullmore E., Sporns O., "Complex brain networks: Graph theoretical analysis of structural and functional systems", Nature Reviews Neuroscience, 10: 186-198, (2009).
26. Bhattacharya J., Petsche H., "Phase synchrony analysis of EEG during music perception reveals changes in functional connectivity due to musical expertise", Signal Processing, 86(12): 3621-3636, (2006).
27. Thayer J.F., Lane R.D., "A model of neurovisceral integration in emotion regulation and dysregulation", Journal of Affective Disorders, 61(3): 201-216, (2000).